[CANCER RESEARCH 60, 896–900, February 15, 2000]

Advances in Brief

p53 Phosphorylation and Association with Murine Double Minute 2, c-Jun NH_2-Terminal Kinase, p14[ARF], and p300/CBP during the Cell Cycle and after Exposure to Ultraviolet Irradiation[1]

Thomas Buschmann, Victor Adler, Ekaterina Matusevich, Serge Y. Fuchs, and Ze'ev Ronai[2]

Ruttenberg Cancer Center, Mount Sinai School of Medicine, New York, New York 10029

Abstract

p53 phosphorylation and association with proteins is implicated in its stability and activity. We have compared the association of DNA-bound and overall pools of p53 with murine double minute 2 (Mdm2), c-Jun NH_2-terminal kinase (JNK), p300/CBP, and p14[ARF] during cell cycle progression. Whereas DNA-bound p53 associates with JNK at G_0-G_1 and with Mdm2 and p300 during S and G_2-M phases, the general pool of p53 was found in complex with JNK and Mdm2 almost throughout the cell cycle. Phosphorylation of p53 at serines 9, 15, and 20 is at the highest levels at G_1 and at serines 37 and 392 during G_2-M phase. Whereas a high dose of UV irradiation was required for phosphorylation of serines 15 and 392 between 8 and 24 h after treatment, a low dose caused immediate phosphorylation on serines 9, 20, and 372. These dynamic changes in the phosphorylation of p53 are expected to play a pivotal role in p53 association, stability, and function.

Introduction

The *p53* tumor suppressor gene encodes a short-lived transcription factor (1, 2), which is stabilized in response to a variety of stresses (3). Posttranslational modifications of p53 by phosphorylation and acetylation have been implicated in its stability and transcriptional activation (3). Among cellular proteins that have been shown to play a direct role in regulating p53 stability and transcriptional activity are Mdm2[3] (4, 5), JNK (6, 7), p14[ARF] (8), and p300/CBP (9). The ability of Mdm2 and JNK to target degradation of p53 is impaired as a result of phosphorylation of p53 by stress kinases, as shown for mitogen-activated protein kinase kinase 1 (6), p38 (10), and ataxia telangiectasia mutant/DNA-protein kinase (11, 12). Whereas ataxia telangiectasia mutant and DNA-protein kinase target p53 phosphorylation at NH_2-terminal residue 15 (12), p38 phosphorylates p53 at the COOH-terminal residue 389 (10), and JNK was reported to phosphorylate p53 at amino acid 34 (13). Other kinases implicated in p53 phosphorylation include casein kinase II, which was shown to phosphorylate amino acid 386, (14) protein kinase C, which phosphorylates p53 on residue 371 (15), and cyclin-dependent kinase 2, which phosphorylates amino acid 315 (16). In addition, acetylation on residues 320 and 373 was observed in response to DNA damage and has been associated with p53 transcriptional activities (17). Although ample reports point to p53 phosphorylation on multiple residues, the requirement(s) and regulation of such phosphorylation is not well understood. Upon activation, p53 induces either growth arrest or apoptosis (18). Although the mechanisms underlying the ability of p53 to elicit such opposing effects are yet to be identified, independent studies point to a different set of p53 regulators and effectors that are affected by p53 in each of these scenarios.

In studying the regulation of p53 stability, we demonstrated previously that, in Swiss 3T3 cells, JNK and Mdm2 target p53 degradation in different phases of the cell cycle (7). In this study, we have compared the association of subpopulations of p53 with proteins implicated in stability and activity of p53 and monitored the pattern of phosphorylation during cell cycle progression and after exposure to UV-C irradiation.

Materials and Methods

Cells and UV Treatment. NHFs (TIG) were kindly provided by Hidetoshi Tahara (NIEHS, Durham, NC) and maintained in DMEM supplemented with 10% fetal bovine serum and antibiotics. Normal human fibroblasts (70% confluent, passages 22–27) were treated with either 9 J/m^2 or 50 J/m^2 UV-C light (254 nm) and harvested at indicated time points.

Cell Lysis, Immunoprecipitation, and Western Blot. Cells were lysed in lysis buffer [20 mM HEPES (pH 7.5), 350 mM NaCl, 25% glycerol, 0.25% NP40, 1 mM sodium vanadate, 0.5 mM phenylmethylsulfonyl fluoride, and 1 μg/ml each of aprotinin, pepstatin, and leupeptin]. Lysates were clarified by centrifugation for 15 min at 14,000 $\times$ *g* at 4°C. The protein concentration was determined, and aliquots were stored at −80°C. For immunoprecipitations, 1 mg of extract at each time point was precleared with 10 μl of protein A/G beads for 1 h at 4°C to remove unspecific binding. Precleared extracts were incubated with either pAb421 or DO1 antibodies overnight at 4°C. Protein A/G beads were added for 3 h at 4°C, and the mixture was then centrifuged at 14,000 rpm for 10 min at 4°C. Protein A/G beads were washed four times with PBS, 3× sample buffer was added, and samples were boiled for 5 min. Eluted material was loaded on an 8% SDS-PAGE and electroblotted, and Western blotting was carried out with the indicated antibodies. For straight Western blot analysis, 150 μg of extracts were loaded on a 8% SDS-PAGE and analyzed as described above.

Western Blot Procedure for Phospho-Antibodies. Cell pellet was lysed with three packed volumes of phospho-extraction buffer [20 mM Tris-HCl (pH 7.5), 20 mM *p*-nitrophenylphosphate, 1 mM EGTA, 50 mM sodium fluoride, 50 μM sodium orthovanadate, 5 mM benzamidine, 100 mM NaCl, 5 mM $MgCl_2$, supplemented with 40 μg/ml DNase I, and 1 μg/ml protease inhibitors] and incubated for 10 min at room temperature. After incubation with sample buffer for 5 min at 95°C, samples (200 μg) were loaded and separated on a 10% SDS-PAGE and electroblotted for 3 h at 100 V. Membrane was incubated with respective acetylation or phospho-antibodies overnight and developed using ECL detection.

EMSA. For gel-shift assays, p53 prepared from NHFs (2 μg) was immunoprecipitated with either DO1 or pAb421 antibodies. Elution of p53 from the respective antibodies was carried out by adding 75 μg of peptides corresponding to the binding site of either DO1 (PPLSQETFSDLWKL) or pAb421 (HLKSKKGQSTSRHK) antibodies on p53. After elution, p53 was concentrated on M_r 30,000 cutoff columns and used for EMSA. A fraction of the eluted and dialyzed p53 was separated on 8% SDS-PAGE, followed by immunoblot analysis to verify that equal amounts of protein are used for gel shift reactions. An equal amount of eluted p53 (20 μl) was mixed with

Received 10/18/99; accepted 12/30/99.

The costs of publication of this article were defrayed in part by the payment of page charges. This article must therefore be hereby marked *advertisement* in accordance with 18 U.S.C. Section 1734 solely to indicate this fact.

[1] Support from NIH Grant CA78419 (to Z. R.) is gratefully acknowledged.

[2] To whom requests for reprints should be addressed, at Ruttenberg Cancer Center, Mount Sinai School of Medicine, 1425 Madison Avenue, Room 15-20, New York, NY 10029. Phone: (212) 659-5571; Fax: (212) 849-2446; E-mail: ronaiz01@doc.mssm.edu.

[3] The abbreviations used are: Mdm2, murine double minute 2; JNK, c-Jun NH_2-terminal kinase; NHF, normal human fibroblast; EMSA, electrophoretic mobility shift assay.

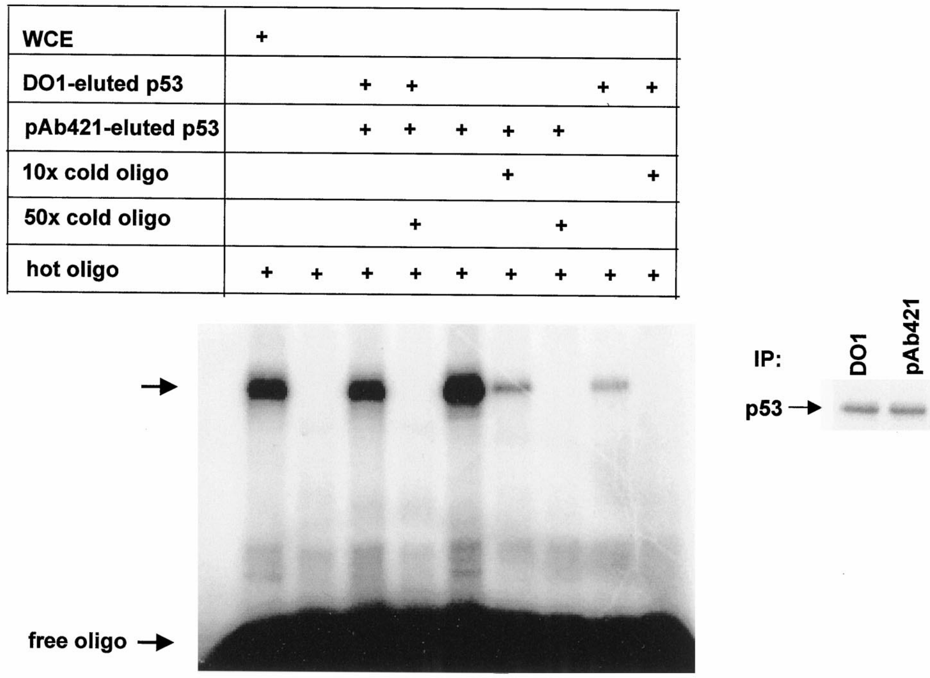

Fig. 1. DNA-binding activity of p53 purified by pAb421 *versus* DO1. Proteins from NHFs were subjected to immunoprecipitation using pAb421 or DO1 antibodies, followed by elution, dialysis, and analysis on Western blots for amounts of p53 (*right panel*). Equal amounts of p53 were taken for gel shift reactions using ^{32}P-labeled oligonucleotide bearing p53 target sequence under conditions indicated in the figure. *oligo*, oligonucleotide; *IP*, immunoprecipitation.

DNA-binding reaction buffer [5× EMSA buffer, 40 mM spermidine, 10 mM DTT, and 500 μg/ml poly(deoxyinosinic-deoxycytidylic acid)] and the ^{32}P-labeled double-stranded oligonucleotide (10 ng/μl ^{32}P probe), which harbors p53 target sequence derived from the human p21/CIP/WAF1 promoter (sense, 5′-AAT TCT CGA GGA ACA TGT CCC AAC ATG TTG CTC GAG-3′; antisense, 5′-CTC GAG CAA CAT GTT GGG ACA TGT TCC TCG AGA ATT-3′). The mixture was incubated for 30 min at room temperature. For competition experiments, excess of unlabeled cold oligonucleotide was added to the reaction. Samples were separated on 4% PAGE, followed by autoradiography.

Results and Discussion

Association of p53 with proteins that alter its stability was carried out in NHFs using pAb421 antibodies, which recognize a DNA-bound form of p53 (19), and DO1 antibodies, which recognize p53 inde-

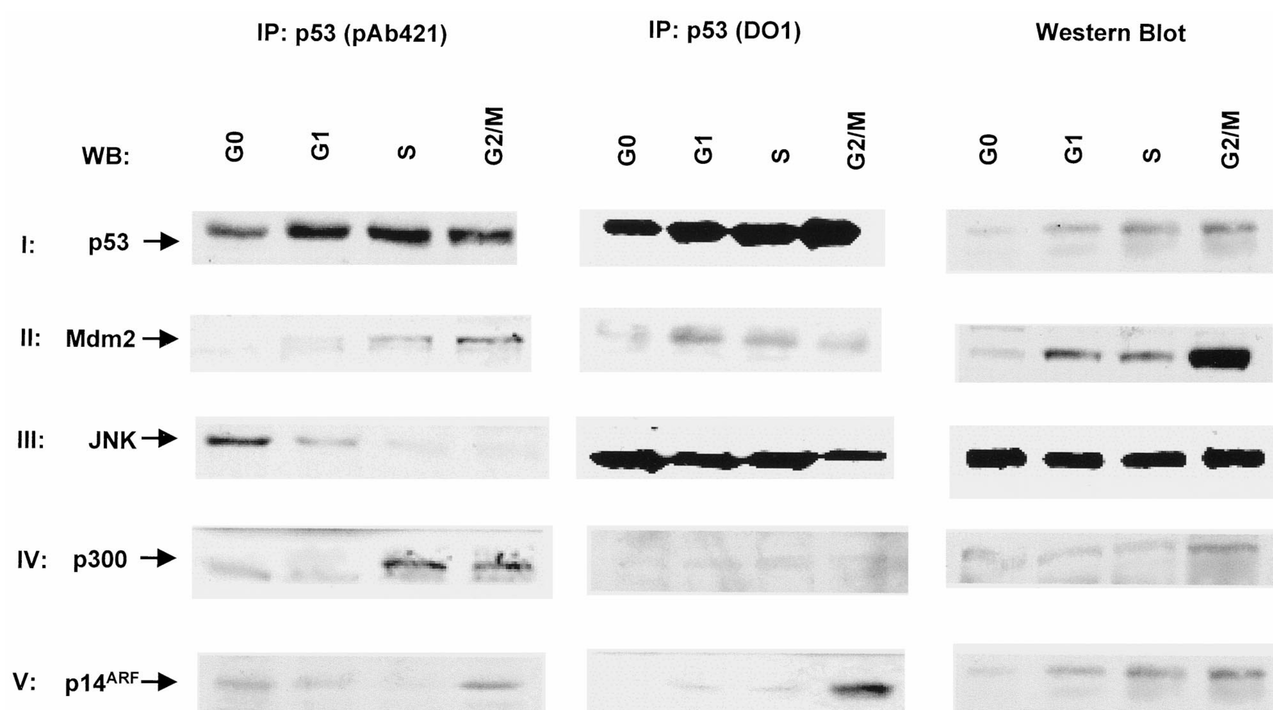

Fig. 2. Association of wild-type p53 with Mdm2, JNK, p300, and p14^{ARF} in different phases of the cell cycle. NHFs at a confluence of 50% were synchronized by maintaining them in medium containing 0.2% calf serum. Upon addition of 10% serum (time 0), cells were harvested at the four phases of the cell cycle based on fluorescence-activated cell sorter analysis to identify the optimal time to represent G_0 (0 h) G_1 (15 h), S (21 h), and G_2-M (27 h). Cells were lysed and incubated for immunoprecipitation (*IP*) with either pAb421 or DO1 antibodies overnight at 4°C. Western blots were carried out with the indicated antibodies. The same analysis was performed using direct Western blot analysis, in which 150 μg of extracts were loaded on an 8% SDS-PAGE and analyzed as described above.

pendent of conformation, and is expected to recognize an overall pool of p53 molecules. Indeed, immunoprecipitations of p53 from NHF cells with each of these antibodies, followed by elution of p53 and analysis of DNA-binding activity, revealed that pAb421-immunoprecipitated forms of p53 exhibit a markedly higher level of DNA-binding activity, when compared with the activity detected in DO1 precipitates (Fig. 1). These findings confirm that pAb421 antibodies recognize a form of p53, which has a greater ability of associating with p53 target sequence. These findings also reveal that the pool of p53 molecules recognized by the DO1 antibodies is different from those detected by pAb421, indicating that these antibodies recognize different subpopulations of p53 molecules.

p53 association with proteins implicated in its stability varied dramatically when pAb421- and DO1-recognized populations of p53 were compared. pAb421-recognized p53 is predominantly associated with Mdm2 in the S and G_2-M phases of the cell cycle, whereas the DO1-recognized p53 was found in complex with Mdm2 throughout the cell cycle with maximal levels during G_1 and S phases (Fig. 2, *II*). Analysis of JNK association with pAb421-recognized p53 identified such a complex during G_0 and G_1 phases (Fig. 2, *III*), as was observed previously in mouse fibroblasts 3T3 cells (7). Although higher, relative levels of JNK bound to the DO1-recognized form of p53 decreased as the cell cycle progressed (Fig. 2, *III*).

Analysis of p300 and p14^{ARF} association with the pAb421-recognizable form of p53 revealed that the amounts of p300 and p14^{ARF} increase continuously as the cell cycle progresses, reaching their highest levels in the G_2-M phase (Fig. 2, *IV* + *V*). The association of p300 with p53 was limited to the pAb421-recognizable form during the late phases of the cell cycle (Fig. 2, *IV*). The association between both pAb421- and DO1-recognized forms of p53 and p14^{ARF} was seen primarily in the G_2-M phase of the cell cycle (Fig. 2, *V*).

These observations suggest that association with each of the proteins that affect p53 stability may require a different conformation of the p53 protein, which is therefore expected to undergo dynamic changes throughout the cell cycle.

The nature of p53 phosphorylation and acetylation was studied using p53 that has been immunoprecipitated with pAb421 antibodies, followed by analysis with antibodies that were raised against specific phosphoacceptor sites. Antibodies that recognize either of the acetylation sites on amino acids 320 and 373 detected the highest levels of acetylation in the G_0 phase, which declined as the cell cycle progressed (Fig. 3*A*). Serines 9, 15, 20, and 372 are phosphorylated in the G_1 phase of the cell cycle (Fig. 3, *B*, *C*, *D*, and *F*). Phosphorylation on Ser-37 was somewhat higher in cells grown in the S and G_2-M phases of the cell cycle (Fig. 3*E*), whereas phosphorylation on Ser-392 was found to occur primarily during the G_2-M phase of the cell cycle (Fig. 3*G*). The active interplay between different sites that are phosphorylated as the cell cycle progresses suggests dynamic changes in the conformation of p53, which in turn, alter affinity for cellular proteins, as demonstrated in Fig. 2. That JNK is immunoprecipitated with pAb421, which also immunoprecipitates the acetylated form of p53, implies that acetylation and JNK association share G_0-related confor-

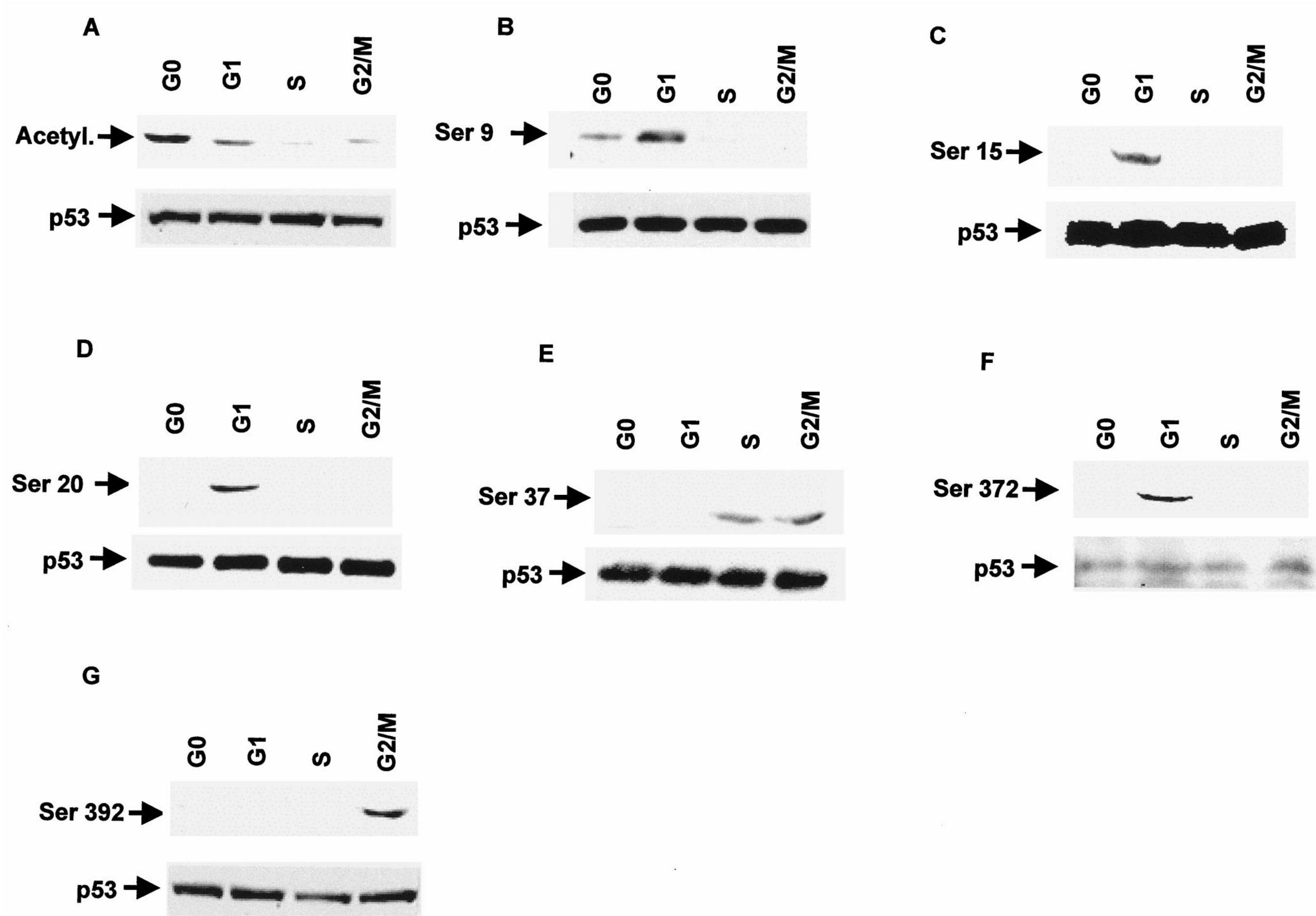

Fig. 3. Acetylation and phosphorylation of p53 at different phases of the cell cycle in NHFs. At time points reflecting G_0, G_1, S, and G_2-M, proteins were prepared from cells, and p53 was immunoprecipitated with pAb421 antibodies. Western blot analysis using acetylation- or phospho-antibodies was carried out (New England Biolabs), and proteins were detected by ECL reaction. *A*, acetylation levels; *B*, Ser-9; *C*, Ser-15; *D*, Ser-20; *E*, Ser-37; *F*, Ser-372; *G*, Ser-392.

mation that is recognized by pAb421. The finding that p14^{ARF} association with pAb421-recognized p53 at G_0 and G_2-M coincides with JNK and Mdm2 association points to possible interplay between the stabilizing and degrading molecules. That substantial lower amounts of JNK and no Mdm2 were found in complex with pAb421-bound p53 during G_1 phase, when most phosphorylation events were recorded, further support the notion that phosphorylation protects transcriptionally active p53 from degradation, as was shown previously (6, 7, 11). Finally, the association of Mdm2 and p300 with active p53 during S-G_2-M phases is in line with recent studies, suggesting that such association is interdependent (9). Together, these data suggest that p53 may elicit an active transcriptional signal at G_1 and G_2-M phases of the cell cycle.

Using phosphospecific antibodies, we elucidated changes in p53 phosphorylation at different time points after the administration of low (9 J/m^2) or high (50 J/m^2) doses of UV irradiation. Lower doses are implicated in p53-elicited growth arrest, whereas high doses reflect p53-mediated apoptosis. Fig. 4*II* depicts the characteristic time-dependent increase in p53 level after UV treatment. Increased phosphorylation on Ser-9 was seen within 1 h after exposure to a high dose of UV irradiation, which has been maintained after 4 and 8 h; after 24 h, the level of Ser-9 phosphorylation decreased (Fig. 4*A*). Exposure to low-dose irradiation led to a weaker yet sustained increase in Ser-9 phosphorylation, even after 24 h. The degree of Ser-9 phosphorylation 1 h after exposure to high-dose UV light was comparable with that seen 24 h after exposure to the low dose (Fig. 4*A*). An increase in Ser-15 phosphorylation was found only after exposure to high-dose irradiation and not earlier than 8 h after treatment (Fig. 4*B*). Phosphorylation of Ser-20 and Ser-37 was induced by both low- and high-dose UV, although the high dose caused a faster and stronger increase in phosphorylation at this site. Whereas the dose of 50 J/m^2 UV light caused the highest level of phosphorylation on Ser-37 after 4 h, exposure to the lower dose led to maximal phosphorylation after 8 h (Fig. 4, *C* and *D*). Both doses of UV elicited maximal phosphorylation on Ser-20 after 4 h (Fig. 4*C*).

The degree of Ser-372 phosphorylation was greater and occurred faster after exposure to high-dose irradiation, although the lower dose also caused a noticeable increase at this phophoacceptor site (Fig. 4*E*). Conversely, Ser-392 was weakly phosphorylated 24 h after high-dose irradiation (Fig. 4*F*). Analysis of p53 acetylation revealed a rapid (1 h) and short-lived increase after exposure to a dose of 50 J/m^2 UV light, whereas the lower dose caused a short-lived increase after 4 h (Fig. 4*G*).

The kinetics of p53 phosphorylation in response to UV irradiation suggest that in NHFs, phosphorylation at Ser-9, -20, -37, and -372 may contribute to p53 stability, whereas phosphorylation on Ser-15 occurs after p53 stabilization took place. The kinetics of p53 Ser-15 phosphorylation is in agreement with Shieh *et al.* (11). It is important to note that earlier phosphorylation of Ser-15 was recorded in other cell systems, including cells of ataxia telangiectasia patients and lymphoblasts (20), suggesting that changes in and contribution of respective phosphoacceptor sites is cell type dependent. In addition, given the complex changes in p53 phosphorylation demonstrated in the present study, it is likely that other phosphoacceptor sites do exist and are crucial for mediating p53 functions. The latter is supported by the recent reports that could not identify major changes in stability/activity of p53 that has been mutated in most of the phosphorylation sites studied here (21).

Overall, our study provides evidence for the existence of at least two subpopulations of p53, which differ in their phosphorylation pattern as in their conformation. Respectively, only a subpopulation of p53, which is recognized here by the pAb421 antibodies, is found to exhibit dynamic changes in association with proteins that contribute to p53 stability and activity and in their phosphorylation pattern. Given

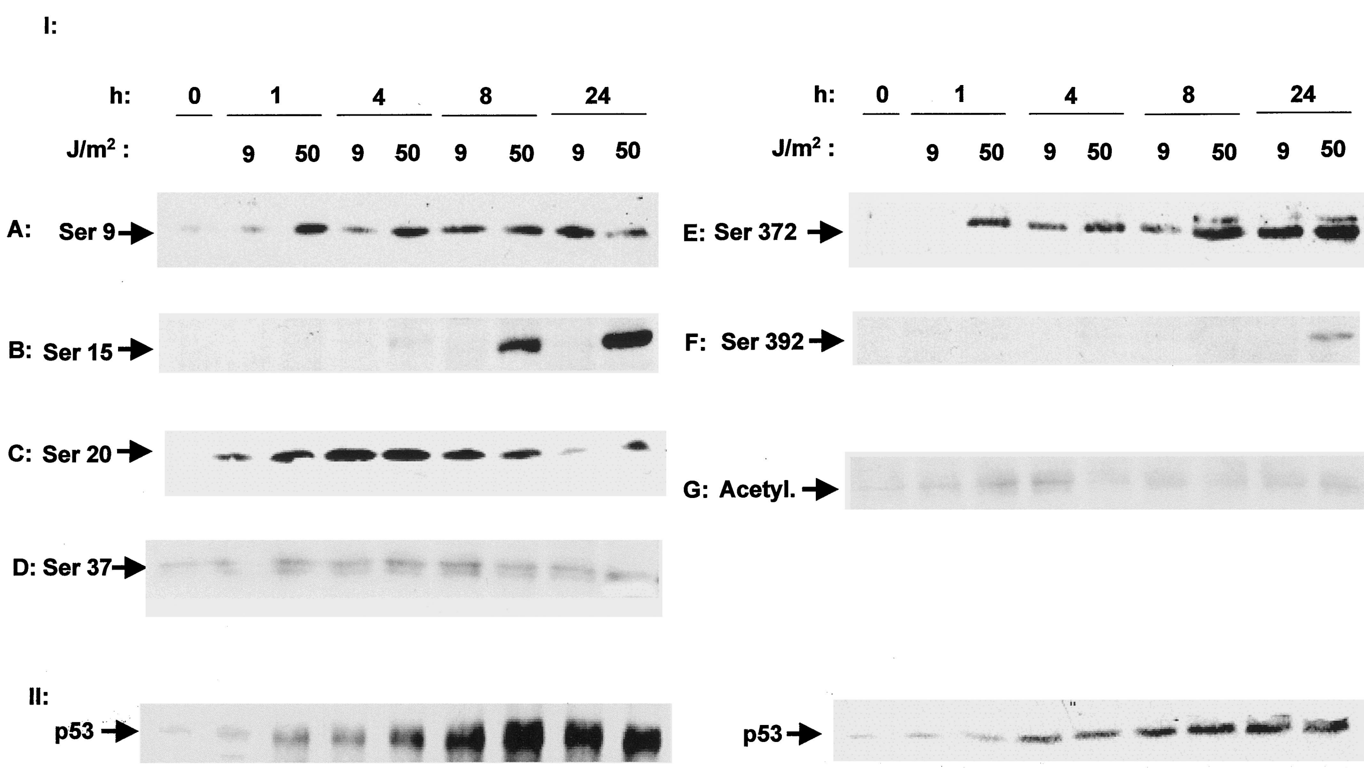

Fig. 4. Acetylation and phosphorylation of p53 after low- or high-dose UV treatment. NHFs (70% confluent) were treated with 9 J/m^2 or 50 J/m^2 UV-C light and harvested at the indicated time points. Cells were lysed and processed as described in "Materials and Methods." *I*, specific immunostaining with different phospho-antibodies directed against the various serine residues. Wild-type p53, shown in *II*, was detected using monoclonal DO1 antibodies (Oncogene).

the abundant support for phosphorylation-dependent changes in p53 conformation, stability, and function, our study identifies changes in p53 association and phosphorylation with cell cycle progression or dose-dependent stress response, thereby breaking down the complex regulation of p53 stability and activity.

Acknowledgments

We thank Thea Tlsty and Moshe Oren for discussion, Michael Comb of New England Biolabs for the phospho-p53 antibodies used in this study, and Hidetoshi Tahara for NHF cells.

References

1. Reich, N., Oren, M., and Levine, A. J. Two distinct mechanisms regulate the levels of a cellular tumor antigen, p53. Mol. Cell. Biol., *3:* 2143–2150, 1983.
2. Hall, P., McKee, P., Menage, H., Dover, R., and Lane, D. P. High levels of p53 protein in UV-irradiated normal human skin. Oncogene, *8:* 203–207, 1993.
3. Meek, D. W. Multiple phosphorylation and the integration of stress signals at p53. Cell Signal, *10:* 159–166, 1998.
4. Haupt, Y., Maya, R., Kazaz, A., and Oren, M. MDM2 promotes the rapid degradation of p53. Nature (Lond.), *387:* 296–299, 1997.
5. Kubbutat, M. H., Jones, S. N., and Vousden, K. H. Regulation of p53 stability by Mdm2. Nature (Lond.), *387:* 299–303, 1997.
6. Fuchs, S. Y., Adler, V., Buschmann, T., Yin, Z., Wu, X., Jones, S. N., and Ronai, Z. JNK targets p53 ubiquitination and degradation in nonstressed cells. Genes Dev., *12:* 2658–2663, 1998.
7. Fuchs, S. Y., Adler, V., Pincus, M. R., and Ronai, Z. MEKK1/JNK signaling stabilizes and activates p53. Proc. Natl. Acad. Sci. USA, *95:* 10541–10546, 1998.
8. Pomerantz, J., Schreiber-Agus, N., Liegeois, N., Silverman, A., Alland, L., Chin, L., Potes, J., Chen, K., Orlow, I., Lee, H., Cordon-Cardo, C., and DePinho, R. The *Ink4a* tumor suppressor gene product, p19Arf, interacts with MDM2 and neutralizes MDM2's inhibition of p53. Cell, *92:* 713–723, 1998.
9. Grossman, S., Perez, M., Kung, A., Joseph, M., Mansur, C., Xizo, Z., Kumar, S., Howley, P. M., and Livingston, D. p300/MDM2 complexes participate in MDM2-mediated p53 degradation. Mol. Cell, *2:* 405–415, 1998.
10. Huang, C., Ma, W., Maxiner, A., Sun, Y., and Dong, Z. p38 kinase mediates UV-induced phosphorylation of p53 protein at serine 389. J. Biol. Chem., *274:* 12229–12235, 1999.
11. Shieh, S., Ikeda, M., Taya, Y., and Prives, C. DNA damage-induced phosphorylation of p53 alleviates inhibition by MDM2. Cell, *91:* 325–334, 1997.
12. Banin, S., Moyal, L., Shieh, S., Taya, Y., Anderson, C. W., Chessa, L., Smorodinsky, N., Prives, C., Reiss, Y., Shiloh, Y., and Ziv, Y. Enhanced phosphorylation of p53 by ATM in response to DNA damage. Science (Washington DC), *281:* 1674–1677, 1998.
13. Milne, D. M., Campbell, L. E., Campbell, D. G., and Meek, D. W. p53 is phosphorylated *in vitro* and *in vivo* by an ultraviolet radiation-induced protein kinase characteristic of the c-Jun kinase, JNK1. J. Biol. Chem., *270:* 5511–5518, 1995.
14. McKendrick, L., Milne, D., and Meek, D. W. Protein kinase CK2-dependent regulation of p53 function: evidence that the phosphorylation status of the serine 386 (CK2) site of p53 is constitutive and stable. Mol. Cell. Biochem., *191:* 187–199, 1999.
15. Chernov, M., Ramana, C., Adler, V., and Stark, G. Stabilization and activation of p53 are regulated independently by different phosphorylation event. Proc. Natl. Acad. Sci. USA, *95:* 2284–2289, 1998.
16. Price, B., Hughes-Davis, L., and Parks, S. Cdk2 kinase phosphorylates serine 315 of human p53 *in vitro*. Oncogene, *11:* 73–80, 1995.
17. Sakaguchi, K., Herrera, J., Saito, S., Miki, T., Bustin, M., Vassilev, A., Anderson, C., and Apella, E. DNA damage activates p53 through a phosphorylation-acetylation cascade. Genes Dev., *12:* 2831–2841, 1998.
18. Canman, C., Gilmer, T., Coutts, S., and Kastan, M. B. Growth factor modulation of p53-mediated growth arrest *versus* apoptosis. Genes Dev., *9:* 600–611, 1995.
19. Halazonetis, T., Davis, L., and Kandil, A. Wild-type p53 adopts a "mutant"-like conformation when bound to DNA. EMBO J., *12:* 1021–1028, 1993.
20. Siliciano, J., Canman, C., Taya, Y., Sakaguchi, K., Apella, E., and Kastan, M. B. DNA damage induces phosphorylation of the amino terminus of p53. Genes Dev., *11:* 3471–3481, 1997.
21. Blattner, C., Tobiasch, E., Litfen, M., Rahmsdorf, H. J., and Herrlich, P. DNA damage induced p53 stabilization: no indication for an involvement of p53 phosphorylation. Oncogene, *18:* 1723–1732, 1999.